Analytic theory of Hund's metals: A renormalization group perspective

Camille Aron and Gabriel Kotliar

Phys. Rev. B **91**, 041110 — Published 12 January 2015

DOI: 10.1103/PhysRevB.91.041110

Analytic theory of Hund's metals: a renormalization group perspective

Camille Aron[1, 2] and Gabriel Kotliar[1]

[1]Department of Physics and Astronomy, Rutgers University, Piscataway, NJ 08854, USA
[2]Department of Electrical Engineering, Princeton University, Princeton, NJ 08544, USA

We study the emergence of quasiparticles in Hund's metals with an $SU(M)\times SU(N)$-symmetric Kondo impurity model carrying both spin and orbital degrees of freedom. We show that the coupling of the impurity spin to the conduction electrons can be *ferromagnetic*, notably for hole-doped iron pnictides. We derive the weak-coupling renormalization group (RG) equations for arbitrary representations of $SU(M)\times SU(N)$. A ferromagnetic spin coupling results in a protracted RG flow, accounting for the surprising particle-hole asymmetry which is observed in the iron-pnictide systems. We establish the low coherence scale $T_{\rm K}$ which depends on the filling through the impurity representation. We also discuss the temperature dependence of the spin and orbital susceptibilities. Finally, we argue that this mechanism explains the strong valence dependence of the coherence scale observed in dilute transition-metal magnetic alloys.

There is renewed interest in a class of materials where strong electronic correlations, manifest in large mass renormalizations, arise from Hund's coupling rather than from the Hubbard U term. Noticeable examples are the recently discovered iron-pnictides and chalcogenides high-temperature superconductors [1, 2], ruthenates [3, 4], or other $4d$ transition-metal oxides [5].

A local approach seems a promising route for the understanding of Hund's metals. GW calculations support the idea that the self-energy at low energies has a purely local character [6]. LDA+DMFT studies, mapping the many-body problem to an impurity problem in a self-consistent determined environment, has provided a successful description of several materials in this class [5]. Hund's metals form a Fermi liquid below a coherence temperature which is remarkably low [1]. The physical degrees of freedom at higher energies are fluctuating moments [7] which are observed in XES measurements [8] and incoherent electronic excitations which are observed in their optical properties [9–11].

Since the DMFT bath of the Hund's metals is relatively structureless at low energies, it is natural to investigate this problem with a representative impurity model, an $SU(M)\times SU(N)$ generalization of the model introduced in Ref. [12] by means of an analytical renormalization group analysis. The goal is to get analytical insights into why is the coherence scale of Hund's metals so low, and what are the physical parameters that control its value. This mystery dates back to the fifties when early investigations of the Kondo temperature $T_{\rm K}$ of dilute transition-metal magnetic alloys revealed that $T_{\rm K}$ decreases dramatically as the d-shell filling approaches half-filling [18, 19]. The renormalization group flows describe an interesting interplay of spin and orbital degrees of freedom, give new insights into why the spin and orbital susceptibility are so different and account for the surprising particle-hole asymmetry observed in the iron-pnictide systems.

Model. We study the impurity model described by the Hamiltonian $H_{\rm K} = H_{\rm bath} + H_{\rm int}$ where $H_{\rm bath} = \sum_{k,m,\sigma} \epsilon_k\, \psi^\dagger_{km\sigma}\psi_{km\sigma}$ describes the non-interacting conduction electrons $\psi_{k\sigma a}$ with momentum k. $\sigma = 1\ldots N$ labels the spin of the electron and $m = 1\ldots M$ labels its orbital. M is the number of active orbitals in the shell (*i.e.* $M=3$ for t_{2g} or $M=5$ for a full shell of d electrons). The physical case for the spin sector is $N=2$ but we keep its value general. We consider a dispersion ϵ_k corresponding to a flat density of states ρ (we later set $\rho=1$ to simplify expressions) with large bandwidth $2D_0$. The spin and orbital degrees of freedom of the impurity, $\boldsymbol{S}$ and $\boldsymbol{T}$, live respectively in faithful representations of $SU(N)$ and $SU(M)$ to be precised below. The coupling to conduction electrons reads (summing over repeated indices)

$$H_{\rm int} = J_{\rm p}\, \psi^\dagger_{a\sigma}\psi_{a\sigma} + J_0\, S^\alpha(\psi^\dagger_{m\sigma}\frac{\sigma^\alpha_{\sigma\sigma'}}{2}\psi_{m\sigma'}) \quad (1)$$
$$+K_0 T^a(\psi^\dagger_{m\sigma}\frac{\tau^a_{mm'}}{2}\psi_{m'\sigma}) + I_0 S^\alpha T^a(\psi^\dagger_{m\sigma}\frac{\sigma^\alpha_{\sigma\sigma'}}{2}\frac{\tau^a_{mm'}}{2}\psi_{m'\sigma'}),$$

with the local conduction electron $\psi_{m\sigma} \equiv \sum_k \psi_{km\sigma}$. $J_{\rm p}$, J_0, K_0, and I_0 are respectively the bare potential, spin-spin, orbital-orbital, and spin-orbital Kondo coupling constants. σ^α ($\alpha = 1\ldots N^2-1$) and τ^a ($a = 1\ldots M^2-1$) are the generators of $SU(N)$ and $SU(M)$ respectively in their fundamental representations. They obey the Lie algebra commutation relations and are normalized such that ${\rm Tr}\left[\sigma^\alpha\sigma^\beta\right] = 2\delta_{\alpha\beta}$ and ${\rm Tr}\left[\tau^a\tau^b\right] = 2\delta_{ab}$. For $SU(2)$ and $SU(3)$, they correspond to the Pauli and Gell-Mann matrices respectively.

We consider the case of Hund's metals with valences n_d less than half-shell filling. Above half-shell capacity, one can perform a particle-hole transformation, before generalizing from $SU(2)$ to $SU(N)$. We denote the distance from half-filling by $d \equiv M - n_d \geq 1$. The effect of strong Hund's coupling is to maximize the impurity spin, therefore we take $\boldsymbol{S}$ as the generators of the totally symmetric representation of n_d fundamental $SU(N)$ spins and $\boldsymbol{T}$ to live in the totally antisymmetric representation composed of $n_d < M$ fundamental $SU(M)$ isospins. See the Young's tableaux in Fig. 1. Notice that at exactly $1/N$-filling, *i.e.* $n_d = M$, the orbital isospin is a sin-

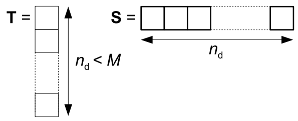

FIG. 1: Young's tableaux of the representations of $\boldsymbol{T}$ and $\boldsymbol{S}$ in our class of Hund's metals. A single box represents a fundamental spin of $SU(M)$ or $SU(N)$.

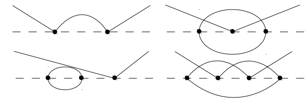

FIG. 2: Above: second and third-order non-parquet diagrams contributing to the RG equations (8)-(10). Below: third-order renormalization of the wave function and a fourth order diagram.

glet state (scalar representation) and the model reduces to an M-channel Coqblin-Schrieffer model with a totally antisymmetric spin representation [21].

The Kondo model in Eq. (1) can be derived, *via* a canonical Schrieffer-Wolff transformation, from the large interaction limit of the $SU(M)\times SU(N)$-symmetric Anderson impurity Hamiltonian [20], $H_{\rm AIM} = H_{\rm imp}+H_{\rm hyb}+H_{\rm bath}$ with

$$H_{\rm imp} \equiv \epsilon_d\, n_d + \frac{1}{2}\sum_{mnpq,\,\sigma\sigma'} U_{mnpq}\, d^\dagger_{m\sigma} d^\dagger_{n\sigma'} d_{p\sigma'} d_{q\sigma}\ , \quad (2)$$

$$H_{\rm hyb} \equiv V \sum_{k,m,\sigma} \psi^\dagger_{km\sigma} d_{m\sigma} + \text{H.c.}\ . \quad (3)$$

$d_{m\sigma}$ represents an impurity electron with spin σ in the orbital m, ϵ_d is the energy level and $n_d \equiv \sum_{m\sigma} d^\dagger_{m\sigma} d_{m\sigma}$. The second term of $H_{\rm imp}$ encodes both Coulombic repulsion and Hund's coupling with $U_{mnpq} \equiv U\delta_{mq}\delta_{np} + J_{\rm H}\delta_{mp}\delta_{nq}$. $H_{\rm hyb}$ is the hybridization with the conduction electrons.

In the large interaction limit, $U \gg D_0 \gg J_{\rm H} \gg V$, the charge degrees of freedom of the Anderson impurity are frozen, and the nominal valence of the impurity is identified to n_d. The states of the impurity carry an $SU(N)$ spin $\boldsymbol{S}$ and an orbital $SU(M)$ isospin $\boldsymbol{T}$ interacting according to $H_{\rm int}$, with the Kondo couplings [22]

$$J_{\rm p} = \frac{1}{MN}\left[\frac{n_d}{\Delta E^-} - \frac{M-n_d}{n_d+1}\frac{N+n_d}{\Delta E^+}\right]V^2\ , \quad (4)$$

$$J_0 = \frac{2}{M}\left[\frac{1}{\Delta E^-} - \frac{M-n_d}{n_d+1}\frac{1}{\Delta E^+}\right]V^2\ , \quad (5)$$

$$K_0 = \frac{2}{N}\left[\frac{1}{\Delta E^-} + \frac{N+n_d}{n_d+1}\frac{1}{\Delta E^+}\right]V^2\ , \quad (6)$$

$$I_0 = 4\left[\frac{1}{n_d}\frac{1}{\Delta E^-} + \frac{1}{n_d+1}\frac{1}{\Delta E^+}\right]V^2\ , \quad (7)$$

in which the virtual charge excitation energies to the $n_d \pm 1$ valence states, $\Delta E^+ \approx \epsilon_d + n_d U$ and $\Delta E^- \simeq -\epsilon_d - (n_d-1)U$, are both positive if $\epsilon_d = -(n_d-1+\alpha)U$ with $\alpha \in]0,1[$. The minus sign in front of the second term of J_0 above implies that, depending on the value of ϵ_d, J_0 can be significantly smaller than the other couplings, and even ferromagnetic, $J_0 < 0$. For $\alpha > \alpha^* \equiv (n_d+1)/(M+1)$ virtual transitions to valence n_d+1 dominate and J_0 is ferromagnetic. For iron pnictites or ruthenates which have $M=5$ or $M=3$ with valences one unit larger than half-filling, a preliminary particle-hole transformation yields $n_d=4$ or $n_d=2$, respectively, and thus hole doping favors a ferromagnetic J_0.

The possibility of such a ferromagnetic spin coupling, is a consequence of the large Hund's coupling encoded in our choice of representations. Indeed, setting $J_{\rm H} = 0$ yields positive Kondo couplings with $J_0 = 2/M\,[1/\Delta E^+ + 1/\Delta E^-]\,V^2$ and $n_d I_0 = 2MJ_0 = 2NK_0$ [22]. In this case, the model reduces to a single-channel Coqblin-Schrieffer model, with a single Kondo coupling $\mathcal{J}_0$ between the conduction electrons and an impurity spin living in the totally antisymmetric representation of $SU(M\times N)$ and composed of n_d electrons.

RG equations. To study the physical properties of the Kondo model, we use a poor man's scaling approach at zero temperature [23, 24]. This consists in reducing the bandwidth by perturbatively integrating over the degrees of freedom of those conduction electrons with an energy in the edge δD of the band and requiring that the physics remain invariant. The corresponding renormalization of the couplings is given by the so-called β functions, $\beta_i \equiv {\rm d}J_i/{\rm d}\ln D$ with $J_i = J, K, I$, together with the initial conditions set by the bare couplings, $J(D_0) = J_0$, $K(D_0) = K_0$ and $I(D_0) = I_0$. The expansion of the β functions to any order in the couplings can be expressed in terms of C_n^S and C_n^T, the eigenvalues of n-th order Casimir invariants of the representations of $\boldsymbol{S}$ and $\boldsymbol{T}$ respectively [28]. Up to third order, we obtain (see Fig. 2)

$$\beta_J = -\frac{N}{2}\left(1-\frac{M}{2}J\right)\left(J^2 + \frac{C_2^T}{2M}I^2\right) + \dots\ , \quad (8)$$

$$\beta_K = -\frac{M}{2}\left(1-\frac{N}{2}K\right)\left(K^2 + \frac{C_2^S}{2N}I^2\right) + \dots\ , \quad (9)$$

$$\beta_I = -\frac{MN}{4}\left[\left(\frac{4}{M}J + \frac{4}{N}K - J^2 - K^2\right)I + \left(\frac{C_3^T}{MC_2^T} + \frac{C_3^S}{NC_2^S}\right)I^2 + \left(\frac{1}{4} - \frac{C_2^T}{2M} - \frac{C_2^S}{2N}\right)I^3\right] + \dots\ . \quad (10)$$

For the sake of generality, we gave the β functions for $\boldsymbol{S}$ and $\boldsymbol{T}$ living in *arbitrary* faithful representations of $SU(N)$ and $SU(M)$. These equations have a broad range of applicability since the spin-orbital Kondo effect can be realized in different settings such as bilayer graphene [16] or nanoscale devices [17]. We shall later return to our particular model by specifying the Casimirs for the Hund's metals.

We discarded the flow of potential scattering since it does not renormalize the other couplings. We also discarded the flow of quadrupolar spin-orbital interactions generated by the pertubative expansion but not initially present in $H_{\rm int}$. For example, the term in $I^2\,(\boldsymbol{S}\cdot\boldsymbol{\sigma})\,(\boldsymbol{Q}\cdot\boldsymbol{\tau})$ with $Q^c \equiv \{T^a, T^b\}{\rm Tr}\left[\tau^{\{a}\tau^b\tau^{c\}}\right]$ was projected on $(\boldsymbol{S}\cdot\boldsymbol{\sigma})\,(\boldsymbol{T}\cdot\boldsymbol{\tau})$ [22] [29].

The six fixed points of the RG Eqs. (8)-(10) are easily identified as (i) $J = K = I = 0$, the non-interacting fixed point, (ii) $J = J^* \equiv 2/M, K = I = 0$, the intermediate-coupling fixed point of the N-channel $SU(M)$ Coqblin-Schrieffer model, (iii) $K = K^* \equiv 2/N, J = I = 0$, the one of the M-channel $SU(N)$ Coqblin-Schrieffer model. (i), (ii) and (iii) are unstable against $J_0 > 0$ or $K_0 > 0$ and, as long as $I_0 = 0$, the RG flows to the fixed point (iv) $J = J^*, K = K^*, I = 0$ which corresponds to the fixed point of two uncoupled multi-channel Coqblin-Schrieffer models and the low-energy physics is dominated by the one with the smallest Kondo scale. As soon as $I_0 \neq 0$, the fixed points (i)-(iv) are all unstable and the RG eventually flows towards (v) $J = J^*, K = K^*, I = I^*_-$ or (vi) $J = J^*, K = K^*, I = I^*_+$ depending on the sign of I_0. Here, $I^*_\pm \equiv \left(a \pm \sqrt{bc + a^2}\right)/b$, with $a \equiv C_3^S/NC_2^S + C_3^T/MC_2^T$, $b \equiv C_2^S/N + C_2^T/M - 1/2$ and $c \equiv 8\left(1/N^2 + 1/M^2\right)$. Contrary to (i)-(iv), the locations of the fixed points (v) and (vi) and the RG flows around them, depend on the representations of the impurity spin $\boldsymbol{S}$ and isospin $\boldsymbol{T}$.

The pertubative expansion of the β functions are only reliable around the non-interacting fixed point (i) and one must be careful before assigning a physical meaning to (v) and (vi). When both sectors, $\boldsymbol{S}$ and $\boldsymbol{T}$, are in their fundamental representation, $C_2^S = (N^2-1)/2N$ and $C_3^S = (N^2-1)(N^2-4)/4N^2$ (and similar expressions for C_2^T and C_3^T), one recovers the β equations derived in [26]. For $SU(2)\times SU(2)$, (v) and (vi) with $I^*_\pm = \pm 4$ are known to be artefacts of the third-order expansion, and the correct fixed point is a strong-coupling fixed point at $I,\ J,\ K \to \infty$. For arbitrary M and N, (v) with $I^*_- = -4\frac{N^2+M^2}{N^2M^2-N^2-M^2}$ is well defined at large N and M and it was conjectured to be stable for all N and M except for $N = M = 2$ [26]. On the other hand, (vi) with $I^*_+ = 4$ lies out of the scope of the pertubative analysis. Kuramoto argued that, similarly to the $SU(2)\times SU(2)$ case, it should be replaced by a strong-coupling fixed point. This is particularly clear at the special values of couplings $2MJ = 2NK = I$ for which the model reduces to the $SU(M\times N)$ Coqblin-Schrieffer model which has only a non-interacting and a strong-coupling fixed point.

RG flow of Hund's metals. We now return to Hund's metals by working with the totally symmetric and antisymmetric representations introduced before (see Fig. 1). The Casimirs read $C_2^S = (N-1)n_d(N+n_d)/2N$, $C_3^S = (N-2)(N-1)n_d(N+n_d)(N+2n_d)/4N^2$, $C_2^T = (M+1)n_d(M-n_d)/2M$, and $C_3^T = (M+2)(M+1)n_d(M-n_d)(M-2n_d)/4M^2$ [27]. Henceforth, we work in the large-N large-M limit while keeping both the ratio $q \equiv M/N$ and the distance to $1/N$-filling, $d \equiv M - n_d \geq 1$, finite. In this limit, the fixed points (v) and (vi) are located at

$$I^*_- \simeq -\frac{4}{NM}\ , \text{ and } I^*_+ \simeq \frac{4}{M}. \tag{11}$$

both lying out the convergence domain of the perturbative expansion [30]. Based on numerical renormalization group results [25] and numerical findings [12], we conjecture that the flow towards (vi) at (J^*, K^*, I^*_+) should be understood as a flow to strong coupling and we use (vi) only to estimate the energy scale at which the Fermi-liquid coherence is restored.

The RG Eqs. (8)-(10) can be solved numerically with arbitrary bare couplings J_0, K_0 and I_0 as initial conditions. Below, we illustrate how the RG trajectories depend on J_0 by solving them analytically in three regimes: weakly ferromagnetic $|J_0| \lesssim K_0$, strongly ferromagnetic $|J_0| \gg K_0$ and strongly antiferromagnetic $J_0 \gg K_0$. Not all these regimes of couplings can be reached from the strong-coupling limit of the multi-band Anderson model, see Eqs. (5)-(7), so that the Kondo model is a more general low-energy model. This is justified because in actual materials there are additional ligand bands contributing to the Kondo couplings.

In the large-M large-N limit and to quadratic order, the RG equations read

$$\beta_J = -N/2\left[J^2 + d/4\ I^2\right] + \dots\ , \tag{12}$$

$$\beta_K = -M/2\left[K^2 + Nq(1+q)/4\ I^2\right] + \dots\ , \tag{13}$$

$$\beta_I = -NI[J + qK + q^2N/4\ I] + \dots\ . \tag{14}$$

To discuss different types of RG flow, we introduce $T_{\rm K}^K \approx \exp(-2/MK_0)D_0$, $T_{\rm K}^I \approx \exp(-4/M^2I_0)D_0$ and $T_{\rm K}^J \approx \exp(-2/NJ_0)D_0$ if $J_0 > 0$ which are the intrinsic Kondo scales in absence of cross-terms in Eqs. (12)-(14). Below, we consider the spin-orbital coupling as the smallest coupling by assuming the hierarchy $T_{\rm K}^I < T_{\rm K}^K$.

Let us first examine the case of a weakly ferromagnetic spin coupling, $J_0 < 0$, with $|J_0| \lesssim K_0$. See Fig. 3(a). At high energies, the terms involving I in the RG Eqs. (12) and (13) can be neglected, thus spin and orbital degrees of freedom are decoupled. The antiferromagnetic coupling K of the totally antisymmetric $SU(M)$ pseudo-spin approaches the non-Fermi-liquid fixed point (ii) controlled by the Kondo scale $T_{\rm K}^K$ and the scaling exponent $\Delta_K \equiv {\rm d}\beta_K/{\rm d}K \approx q$ [21] while the ferromagnetic coupling J of the totally symmetric $SU(N)$ spin slowly flows to weak coupling with an exponent $\Delta_J \equiv {\rm d}\beta_J/{\rm d}J \approx 0$. At energy scales of the order of $T_{\rm K}^K$, J is still ferromagnetic while K reaches its fixed point, $K(T_{\rm K}^K) \approx K^*$. Below $T_{\rm K}^K$, K^* controls $\beta_I \approx -MK^*I < 0$ and the spin-orbital coupling renormalizes to strong coupling, $I(T_{\rm K}^K) \approx I^*_+$. Then, the I^2 term in Eq. (12) drives the growth of J which crosses over from a ferromagnetic to an antiferromagnetic value. The integration of Eq. (12) provides an

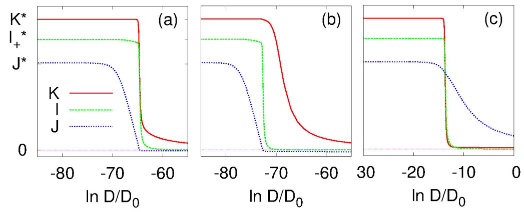

FIG. 3: Numerical RG flow starting from (a) weakly ferromagnetic $|J_0| = 10^{-3} \lesssim K_0$, (b) strongly ferromagnetic $|J_0| = 10^{-1} \gg K_0$, and (c) strongly antiferromagnetic $J_0 = 10^{-2} \gg K_0$. ($q = 3/2$, $d = 1$, $K_0 = 10^{-3}$, $I_0 = 10^{-5}$, $N = 20$).

estimate of the typical energy scale $T_{\rm K}$ at which $J \to J^*$, *i.e.* at which the strong-coupling regime establishes,

$$T_{\rm K}(d) \approx \exp\left(-q/d\right) T_{\rm K}^K \ . \qquad (15)$$

Note that Eq. (15) is still valid for a relatively small antiferromagnetic coupling, as long as $T_{\rm K}^J < T_{\rm K}^K$ or $T_{\rm K}^J < T_{\rm K}^I$. In agreement with the experimental and numerical evidence, $T_{\rm K}$ is found to decrease as one approaches $1/N$-filling (*i.e.* as d gets smaller). At a more formal level, $T_{\rm K}$ depends *explicitly* on the representations of the spin and the orbital isospin. This is unlike the typical Kondo scales emerging in Kondo models without spin-orbital coupling.

Let us now discuss the scenario with large ferromagnetic coupling $|J_0| \gg K_0$. See Fig. 3(b). As seen in Eq. (14), J controls the renormalization of I as long as $K \ll |J|$ and $\beta_I \approx -NJI > 0$. Thus, I first slowly renormalizes to weak coupling and reaches values on the order of $I_0' \equiv q^2 I_0 K_0^2/|J_0|^2 \ll I_0$ at $T_{\rm K}^K$ (when $K \to K^*$). The subsequent growth of I to I_+^* is therefore delayed by such a small initial value and I escapes weak coupling at a scale $I_0'^{-1/\Delta_I} T_{\rm K}^K < T_{\rm K}^K$ with $\Delta_I \equiv {\rm d}\beta_I/{\rm d}I \approx -2q$. In turn, this also delays the subsequent renormalization of J to J^*. The relevance of multi-channel Kondo physics for the intermediate asymptotics was conjectured and the operator responsible for the crossover to the Fermi liquid at low energies was identified in [13].

It is useful to contrast the scenarios above with the case of large antiferromagnetic coupling $J_0 \gg K_0$. See Fig. 3(c). There, the RG flow is radically different as all three couplings reach strong coupling concomitantly at the scale set by $T_{\rm K}^J > T_{\rm K}^K$.

Finally, our results can also be compared to the case of the absence of Hund's coupling, $J_{\rm H} = 0$, for which the model reduces to the antiferromagnetic $SU(M \times N)$ Coqblin-Schrieffer model described before. There, all antiferromagnetic Kondo couplings are locked together by symmetry considerations and strong coupling is reached at energies on the order of $\exp\left[-2/(MN\mathcal{J}_0)\right] D_0$.

Susceptibilities. The RG flow can be used to study physical observables such as the impurity spin and orbital static susceptibilities, χ_S and χ_T respectively. The temperature scaling equations derived in [22] have solutions

$$\chi_{S/T}(T) \sim \frac{1}{T} \exp\left(- \int_T^{D_0} \frac{{\rm d}D}{D} \gamma_{S/T}\left(J_i(D)\right) \right) , \qquad (16)$$

with the functions $\gamma_S = MN(J^2 + C_2^T I^2/2)/2$ and $\gamma_T = MN(K^2 + C_2^S I^2/2)/2$. Let us focus on the ferromagnetic case, $J_0 < 0$. At high temperatures $T \sim D_0$, the exponent above can be neglected and both susceptibilities follow a Curie law, *i.e.* $1/T$. At temperatures down to $T_{\rm K}^K$, Eq. (16) and the RG flow discussed above imply that the magnitude of χ_T is significantly smaller than the one of χ_S. At $T_{\rm K}^K$, the orbital susceptibility crosses over to a strong-coupling regime and $\chi_T \to 0$ when $T \to 0$. In the weakly ferromagnetic scenario $|J_0| \lesssim K_0$, $\gamma_S(T_{\rm K}^K)$ is controlled by I_+^* thus the spin susceptibility crosses over to strong coupling concomitantly with χ_T. However, in the strongly ferromagnetic case $|J_0| \gg K_0$, the retardation of $I \to I_+^*$ over $K \to K^*$ leads to a crossover of χ_S at even lower temperatures. These findings are consistent with the numerical results of [12] and provide a simple picture of the incoherent regime of Hund's metals at intermediate energy scales: composite quasiparticles incorporate orbital degrees of freedom but not spin degrees of freedom, screening $\boldsymbol{T}$ but not $\boldsymbol{S}$.

Discussion. We studied impurities in the presence of strong Hund's coupling in terms of a Kondo problem with spin and orbital degrees of freedom. The spin coupling can be ferromagnetic or antiferromagnetic depending on the filling of the underlying Anderson impurity model. In the Hund's metal region, very close to half-filling the coupling is ferromagnetic and this is the regime that corresponds to hole-doped iron pnictides, while the antiferromagnetic case is realized in the strongly electron-doped regime. In the ferromagnetic case, there is a subtle interplay of spin and orbital degrees of freedom which leads to protracted flows until the Fermi liquid. This explains the strong doping dependence of the coherence scale that has been observed, the electron-doped iron pnictides such as $Fe_{1-x}Co_xBa_2As_2$ [14] having a much larger coherence temperature than hole-doped materials such as KFe_2As_2 [15].

Finally, our Kondo impurity model describes true magnetic impurities with large Hund's coupling and embedded in metallic hosts. Thus the above mechanism also applies to dilute transition-metal magnetic alloys and successfully reproduces the overall trend of the experimentally measured coherence temperature as a function of filling [18].

We are grateful to N. Andrei, J. von Delft, K. Haule, M. Kharitonov, K. Stadler and A.M. Tsvelik for insightful discussions. This work has been supported by NSF grants No. DMR-0906943 and DMR-115181.

[1] K. Haule and G. Kotliar, New J. Phys. **11**, 025021 (2009).
[2] Z.P. Yin, K. Haule, and G. Kotliar, Nat. Phys. **7**, 294 (2011).
[3] P. Werner, E. Gull, M. Troyer, and A.J. Millis, Phys. Rev. Lett. **101**, 166405 (2008).
[4] J. Mravlje *et al.*, Phys. Rev. Lett. **106**, 096401 (2011).
[5] L. de Medici, J. Mravlje, and A. Georges, Phys. Rev. Lett. **107**, 256401 (2011); Annu. Rev. Condens. Matter Phys. **4**, 137-178 (2013).
[6] J.M. Tomczak, M. van Schilfgaarde, and G. Kotliar, Phys. Rev. Lett. **109**, 237010 (2012).
[7] P. Hansmann, R. Arita, A. Toschi, S. Sakai, G. Sangiovanni, and K. Held, Phys. Rev. Lett. **104**, 197002 (2010).
[8] H. Gretarsson *et al.*, Phys. Rev. B **84**, 100509(R) (2011).
[9] A.A. Schafgans et al., Phys. Rev. Lett. **108**, 147002 (2012).
[10] T. Katsufuji, M. Kasai, and Y. Tokura, Phys. Rev. Lett. **76**, 126 (1996).
[11] Y. S. Lee *et al.*, Phys. Rev. B **67**, 113101 (2003).
[12] Z.P. Yin, K. Haule, and G. Kotliar, Phys. Rev. B **86**, 195141 (2012).
[13] S. Akhanjee and A.M Tsvelik, Phys. Rev. B **87** 195137 (2013).
[14] F. Rullier-Albenque *et al.*, Phys. Rev. Lett. **103**, 057001 (2009).
[15] F. Hardy *et al.*, Phys. Rev. Lett. **111**, 027002 (2013).
[16] M. Kharitonov and G. Kotliar, Phys. Rev. B **88**, 201103 (2013).
[17] P. Jarillo-Herrero, J. Kong, H.S.J van der Zant, C. Dekker, L.P. Kouwenhoven, S. De Franceschi, Nature **434**, 484 (2005).
[18] M.D. Daybell and W.A. Steyert, Rev. Mod. Phys. **40**, 380 (1968).
[19] J.R. Schrieffer, J. Appl. Phys. **38**, 1143 (1967).
[20] R.H. Parmenter, Phys. Rev. B **8**, 1273 (1973).
[21] O. Parcollet *et al.*, Phys. Rev. B **58**, 3794 (1998).
[22] See the supplementary material.
[23] P.W. Anderson, J. Phys. C **3**, 2439 (1970).
[24] J. Sólyom, Fundamentals of the Physics of Solids, Vol. 3, Springer (2011).
[25] Y. Nishikawa, D.J.G. Crow, and A.C. Hewson, Phys. Rev. B **82**, 245109 (2010).
[26] Y. Kuramoto, Eur. Phys. J. B **5**, 457 (1998).
[27] S. Okubo, Phys. Rev. D **16**, 3528 (1977).
[28] $C_n^S\,\mathbb{I}_S \equiv \mathrm{Tr}[\frac{\sigma^{\{\alpha_1}}{2}\ldots\frac{\sigma^{\alpha_n\}}}{2}]S^{\alpha_1}\ldots S^{\alpha_n}$ where $\mathbb{I}_S$ is the identity in the representation of $\boldsymbol{S}$ and $\{a_1\ldots a_n\}$ stands for the sum over all permutations weighted by $1/n!$.
[29] In the fundamental representations, quadrupolar terms are simply absent since one necessarily has $\boldsymbol{Q}\propto\boldsymbol{S}$ owing to the fact that $\{\mathbb{I},S^a;a=1\ldots N^2-1\}$ is a complete basis of the $SU(N)$ operators.
[30] A rapid inspection shows that the higher order terms in the expansion of β_I scale as $N^{2n-2}I^n$ for $n\geq 4$ (see *e.g.* the fourth order term in Fig. 2). This indicates that the pertubative expansion converges if $|I|\ll 1/N^2$.